Dissociation of spin objects in geometrically frustrated $CdFe_2O_4$

K. Kamazawa,[1] S. Park,[2,3] S.-H. Lee,[2] T. J. Sato,[2] and Y. Tsunoda[1]
[1]*Department of Applied Physics, School of Science and Engineering, Waseda University, 3-4-1, Ohkubo, Shinjuku-ku, Tokyo, 169-8555 Japan*
[2]*NIST Center for Neutron Research, National Institute of Standards and Technology, Gaithersburg, Maryland 20899, USA*
[3]*Department of Materials Science and Engineering, University of Maryland, College Park, Maryland 20742, USA*
(Received 14 March 2004; published 27 July 2004)

Using inelastic neutron scattering, we measured the diffuse scattering pattern of the geometrically frustrated $^{110}CdFe_2O_4$. The observed pattern resembles that of $ZnCr_2O_4$, indicative of strong nearest-neighbor antiferromagnetic correlations in contrast to the ferromagnetic nearest neighbor interactions of the isomorphic $ZnFe_2O_4$. This result demonstrates that the subtle 90° Fe^{3+}-O-Fe^{3+} interaction changes its nature by chemical pressure. Meanwhile, the temperature dependence of the diffuse scattering shows hexagonal spin objects decay very gradually with increasing temperature and can be seen even at temperature as high as five times Curie-Weiss temperature. At low temperatures, spin freezing with only short-range correlations is observed associated with 13 K susceptibility anomaly. No long-range order is found down to 0.1 K with applied field of up to 9 T.

DOI: 10.1103/PhysRevB.70.024418 PACS number(s): 75.50.Ee, 75.40.Gb, 75.50.Lk

$CdFe_2O_4$ has the normal spinel structure AB_2O_4, which belongs to the cubic space group $Fd\bar{3}m$. Its octahedral *B* site ions, Fe^{3+}, form the three-dimensional network of corner-sharing tetrahedra, the famous lattice known for strong geometrical frustration when its vertices are occupied by spins with antiferromagnetic (AF) nearest-neighbor interactions or ferromagnetic (FM) interactions with uniaxial anisotropy. The same network is also found in pyrochlores of general formula $A_2B_2O_7$ and cubic *C*15 Laves phase compounds AB_2 such as $Y(Sc)Mn_2$.[1]

Geometrical frustration in such systems usually manifests itself through suppression of long-range order (LRO) to a temperature well below Curie-Weiss temperature Θ_{CW} and strong spin fluctuations originating from zero modes. In addition exotic phases are often found instead of Néel order at low temperatures. For example, $Tb_2Ti_2O_7$ is a spin liquid,[2] $Y_2Mo_2O_7$ a spin glass,[3–5] ferromagnetic $Ho_2Ti_2O_7$ a spin ice due to uniaxial anisotropy.[6] Even heavy fermionic behavior can be found in *d*-electron LiV_2O_4.[7]

Meanwhile, theoretical work on such spin systems on the network of corner sharing tetrahedra with nearest AF interactions so far all predict spin liquid phase with large entropy at low temperatures instead of LRO.[8–10] In many real systems, however, the third law of thermodynamics responds to the macroscopically degenerate ground state of the geometrically frustrated systems through small perturbations such as further-nearest-neighbor interactions or magnetoelastic coupling, which relives frustration and lifts degeneracy. Study of such small perturbations and onset of low temperature ordered phase is an important field of research.

Take $ZnCr_2O_4$ for example. Strong geometrical frustration in this material is evidenced by a very low $T_c = 12.5$ K to an AF phase compared to large $\Theta_{CW} = -390$ K.[11] Moreover, recent success in identifying local zero energy modes makes it a very good model system with nearest-neighbor Heisenberg AF interactions.[12] This has led to a growing interest in magnetic *B* site spinels. Recently some of us conducted neutron scattering experiments on another spinel $ZnFe_2O_4$ and observed its diffuse scattering pattern from the frustrated spin system. Compared to a Cr^{3+} ion which has three t_{2g} electrons and dominant-nearest neighbor interactions through direct coupling, a Fe^{3+} ion contains additional two e_g electrons whose orbital extends toward surrounding oxygen ions, making further neighbor interactions more likely in ferrite spinels. Hence it was questioned whether $ZnFe_2O_4$ would show different behavior than $ZnCr_2O_4$. Indeed these additional electrons are shown to play a significant role in modifying the magnetic diffuse scattering pattern.[13,14] To better understand the behaviors of ferrite spinels, we investigated $CdFe_2O_4$, an end member of Co-Cd ferrites with larger nonmagnetic Cd^{2+} ions than Zn^{2+} ions, using the inelastic neutron scattering technique.

Due to the highly neutron-absorbing nature of Cd, however, study of spin fluctuations has not been available to date for $CdFe_2O_4$. Here we report a neutron scattering measurement on $CdFe_2O_4$ single crystals grown with ^{110}Cd isotope. We observed that the diffuse magnetic scattering pattern arising from geometrical frustration is dramatically different than that of $ZnFe_2O_4$ but resembles the $ZnCr_2O_4$ pattern indicating nearest-neighbor AF correlations. This pattern, which originates from hexagonal spin clusters, persists to a surprisingly high temperature, enabling us to study its gradual decay up to 5 times Θ_{CW}. Also our good quality single crystal $CdFe_2O_4$ showed no LRO down to 0.1 K under the applied field of 9 T. Instead, short-range ordered state developed upon cooling at low temperatures.

$CdFe_2O_4$ single crystals were grown by flux method using more than 90% of ^{110}Cd. Naturally abundant and highly neutron-absorbing ^{113}Cd content was kept at about 0.01%. Single crystals grown from the same batch had the shape of octahedra with their edges sized at 5–7 mm. The lattice constant was measured at an ambient temperature using the powder x-ray diffraction. The determined value of 8.715 Å is in good agreement with previous measurement.[15]

The bulk magnetic behavior was checked through magnetic susceptibility measurement of a single crystal using a

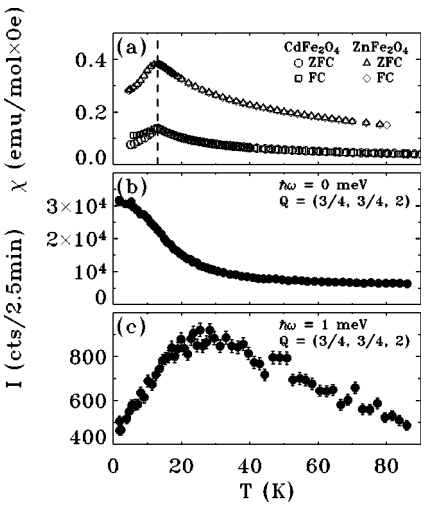

FIG. 1. Temperature dependence of the magnetic susceptibility and neutron scattering order parameters. (a) Bulk magnetic susceptibility of $CdFe_2O_4$ measured at 200 G in zero field cooling (ZFC) (○) and field cooling (FC) (□) conditions. Also plotted are $ZnFe_2O_4$ magnetic susceptibility in ZFC (△) and FC (◇)conditions with the applied field of 500 G. Dashed line signifies the transition temperature common to the two ferrites. (b) Elastic scattering intensity as a function of temperature measured at $Q=(3/4,3/4,2)$. (c) Inelastic scattering intensity at the same Q but with energy transfer of $\hbar\omega=1$ meV.

Quantum Design SQUID with the applied field of 200 G along the [001] direction. Figure 1(a) displays the magnetic susceptibility of $CdFe_2O_4$ along with the previously published $ZnFe_2O_4$ result.[14] No thermal hysteresis was found in both field cooled (FC) and zero field cooled (ZFC) processes suggesting the system does not become glassy at low temperatures. The little split between the FC and ZFC data is believed to be from sample imperfection.[16] Θ_{CW} and the magnetic moment inferred from the high-temperature susceptibility curve are −53 K and $4.44\mu_B$, respectively. The susceptibility shows an anomaly at $T_f=13$ K—probably a sign of transition to an ordered state. Since the absolute value of Θ_{CW} is much larger than T_f, strong geometrical frustration is expected. The estimated exchange constant $J=[3k_B\Theta_{CW}/zS(S+1)]$ of 5.9 meV is obtained assuming nearest-neighbor interactions only with the coordination number z set to 6. Although both susceptibility curves look similar, $ZnFe_2O_4$ has positive $\Theta_{CW}\sim100$ K when the high-temperature susceptibility is considered, suggesting dominant ferromagnetic correlations between Fe^{3+} ions of $ZnFe_2O_4$.[14]

Neutron scattering measurement on $CdFe_2O_4$ was performed on SPINS triple axis spectrometer installed at a cold neutron guide at NIST Center for Neutron Research. To enhance data collection rate, four single crystals of net mass ~1 g were comounted on the (h h l) scattering plane and the seven 2.1 cm wide horizontally focusing analyzer blades were used at a fixed final energy $E_f=5.1$ meV along with a cooled Be filter to suppress higher order neutrons. Field measurement was carried out using the two comounted crystals on the (h k 0) scattering plane using 12 T vertical field magnet with dilution refrigerator.

Figures 1(b) and 1(c) shows temperature dependence of elastic and inelastic scattering at the wave vector transfer $Q=(3/4,3/4,2)$ where strong elastic scattering is observed at low temperatures. No sharp magnetic Bragg peak is detected associated with the 13 K susceptibility anomaly, indicating that the anomaly is not associated with LRO as previously believed.[15] The plotted elastic signal is part of the wider-than-resolution diffuse magnetic peak and it decays gradually upon heating, which is consistent with the finite energy resolution of the spectrometer. Applying 9 T field along [001] direction had no effect on the shape of the order parameter curve indicating that the freezing temperature remains about the same as in the zero field case. The inelastic signal at the energy transfer of 1 meV featured a broad peak centered at ~30 K showing the shift of the spectral weight to the elastic channel with the decreasing temperature.

Although $CdFe_2O_4$ shares the same magnetic Fe^{3+} ions with the isomorphic $ZnFe_2O_4$, the magnetic diffuse scattering patterns show big difference between the two (see Figs. 2 and 5. Previously $ZnFe_2O_4$ was found to have strong magnetic diffuse scattering at (3/4, 3/4, 0), (5/4, 5/4, 2), and (1/4, 1/4, 1). Meanwhile our $CdFe_2O_4$ measurement shows distinct inelastic neutron scattering peaks at (5/4, 5/4, 0) and (3/4, 3/4, 2) at $\hbar\omega=1$ meV energy transfer as shown in Fig. 2(a). The latter locations coincides with $ZnCr_2O_4$ excitation peaks with very similar intensity map. Thus $CdFe_2O_4$ diffuse scattering pattern can be modeled in the same manner as in the case of $ZnCr_2O_4$, i.e., it is believed to represent local zero energy modes stemming from the space-filling collinear AF hexagons.[12]

What is more intriguing is the fact that this pattern persists at much higher temperatures than Θ_{CW}. Data taken at 270 K ($\sim5\Theta_{CW}$) is shown in Fig. 2(b). Although strong paramagnetic scattering dominates low momentum transfer portion of the plot, two peaks at (±3/4, ±3/4, 2) are still seen at this temperature.

To characterize the evolution of $CdFe_2O_4$ diffuse scattering observed at (3/4, 3/4, 2) more closely, constant E scans and constant Q scans were performed at several temperatures. Figures 3(a)–3(c) shows the constant E scans along [110] direction at an energy transfer of 1 meV. Two diffuse peaks (±3/4, ±3/4, 2) are covered in those scans. The solid curve is the result of fits to a double Lorentzian convoluted with the instrumental resolution. At all temperatures the peak width is clearly wider than the resolution represented by the horizontal solid bars under the peaks, evidencing short range dynamic correlations. The constant Q scans [Figs. 3(d)–3(f)] show gradual increase of the inelastic scattering signal upon cooling down to 30 K. When further cooled below 30 K, spectral weight shifts from the inelastic channel to the elastic channel noticeably. These energy scans can be fit to the single imaginary pole susceptibility $S(Q,\omega)=\chi''(\omega)[1+n(\omega)]$ with $\chi''(\omega)=\chi_0\omega\Gamma/(\omega^2+\Gamma^2)$ and $n(\omega)=[\exp(\hbar\omega/k_BT-1)]^{-1}$ where Γ is the relaxation rate. Eventually at low temperatures, local resonance develops as indicated by the arrow in Fig. 3(f). Although no structural change was observed experimentally, it is a strong indication that certain anisotropy develops that contributes to the establishment of the observed short-range order.

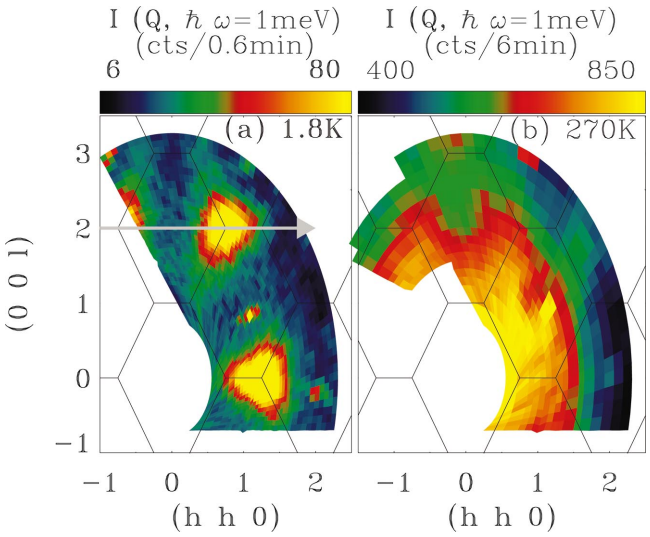

FIG. 2. (Color) $CdFe_2O_4$ diffuse scattering pattern on the $(1\bar{1}0)$ scattering plane at (a) 1.8 Kand (b) 270 K at $\hbar\omega=1$ meV. The gray arrow corresponds to the direction of the constant E scans shown in Fig. 3.

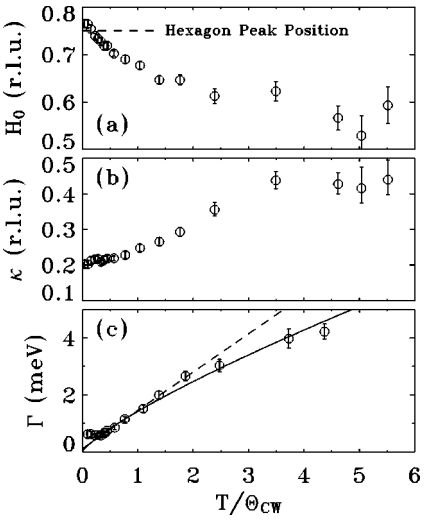

FIG. 4. Temperature dependence of the fit parameters. (a) The peak position H_0. (b) The intrinsic line width κ. (c) The relaxation rate Γ obtained by fitting the energy spectrum. The curves are fits to the relaxation rate as described in the text.

Fit parameters from constant E scans as well as constant Q scans are summarized as a function of temperature in Fig. 4. Having established that the hexagonal spin clusters—the smallest of the string modes[17]—dominate the low-temperature dynamics of $CdFe_2O_4$, the temperature dependence study of its diffuse scattering pattern provides a glimpse of how the dynamic modes evolve with increasing temperature. Figure 4(a) shows the incommensurate diffuse scattering peak position H_0, characteristic of geometrical frustration. Upon heating H_0 is seen to shift slightly toward a small Q value away from the hexagonal mode peak position. Meanwhile, intrinsic line width κ shown in Fig. 4(b) increases with increasing temperature indicating reduced correlation length. The correlation length ξ inferred from the intrinsic line width is 2.2(2)Å at room temperature, smaller than the nearest-neighbor distance between Fe^{3+} ions $d_{\text{Fe-Fe}}=3.081$ Å, while it is 4.9(3)Å at 1.5 K—about 1.6 $d_{\text{Fe-Fe}}$. Similar decrease of the correlation length with increasing temperature was observed from $ZnCr_2O_4$.[12]

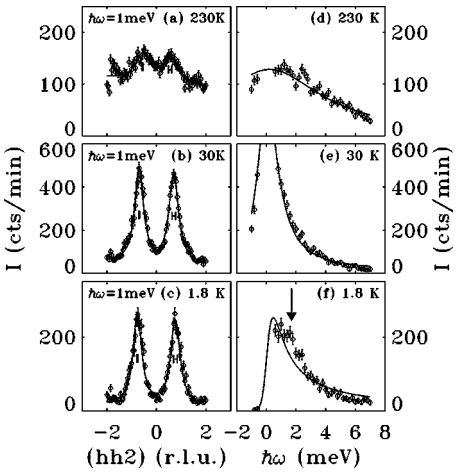

FIG. 3. Inelastic neutron scattering intensity around (±3/4, ±3/4, 2). (a)–(c) Constant E scans along [110] direction at 240, 30, and 1.8 K. The horizontal bars indicate the instrumental resolution at (±3/4, ±3/4, 2). (d)–(f) Constant Q scans at (3/4, 3/4, 2) at 230, 30, and 1.8 K, respectively. The temperature independent background was subtracted and the resolution limited elastic peak was removed from the data. The solid fitting curves in the plots are explained in the text.

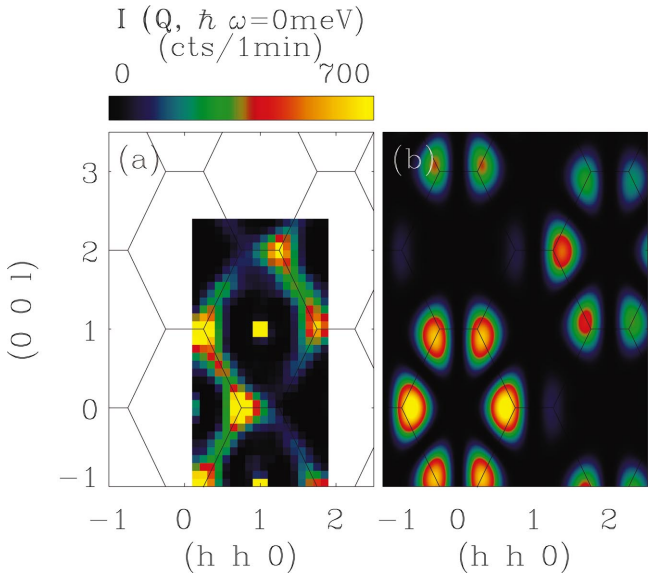

FIG. 5. (Color) (a) $ZnFe_2O_4$ elastic diffuse scattering pattern on the (h h l) scattering plane at 1.5 K. The measurement was taken place on the HQR triple axis spectrometer installed at a thermal guide of JRR-3M, Tokai, Japan (Ref. 14). (b) Computed contour maps using Eq. (1).

The temperature dependence of the relaxation rate Γ obtained from fitting the constant Q scans is plotted in Fig. 4(c). As typically found in geometrically frustrated magnets Γ decreases upon cooling due to slowing spin dynamics. It also shows approximately linear temperature dependence between T_f and 100 K $\sim 2\Theta_{CW}$ and non-vanishing Γ below T_f. For spin glass systems Γ softens at a finite T_g as in the case of $Y_2Mo_2O_7$.[4] Even when extrapolation of the linear fit to the selected temperature range data above T_f is carried out, an abscissa is found very close to the origin as shown as broken lines in Fig. 4(c). Hence 13 K susceptibility anomaly of $CdFe_2O_4$ does not seem to be associated with a spin glass transition. Rather, linearly increasing Γ with the temperature above T_f is in accordance with the theories of spin liquid state.[9,10] When Γ in the entire temperature range is used for fitting with T^{α}, the exponent $\alpha = 0.79(4)$ is produced [solid curve in Fig. 4(c)]. For $ZnCr_2O_4$, α has the value of 0.81(4).[11] It was argued that the smaller than the unity exponent for $ZnCr_2O_4$ may have been due to the sudden onset of long-range order at T_c.[11] In a similar note, formation of static short-range order (SRO) below T_f might be responsible for less than unity α of $CdFe_2O_4$.

We have seen that $CdFe_2O_4$ resembles $ZnCr_2O_4$ in a number of ways despite they undergo seemingly different types of phase transitions at respective freezing temperature. Not only they share almost identical diffuse scattering pattern, but also their temperature dependence, notably the dynamical correlation length obtained from the intrinsic line width and the spin relaxation rate, behave in a very similar fashion. All of these indicate the magnetic properties of $CdFe_2O_4$ is governed by the geometrical frustration due to the nearest-neighbor AF interactions between Fe^{3+} magnetic moments. In addition, decreasing H_0 and increasing κ as a function of temperature as shown in Figs. 4(a) and 4(b) provides an important clue on how the dynamics change with temperature. With increasing T and decreasing ξ, spins are not expected to form large spin clusters any more, i.e., the hexagonal spin clusters begin to dissociate. As the ξ becomes smaller than the nearest neighbor distance, it is expected that the diffuse scattering from the nearest neighboring AF correlations dominate at high temperatures. One possibility is to find a diffuse scattering pattern observed in a spin liquid $Tb_2Ti_2O_7$.[2] Thus it is surprising to find that the hexagon peaks persist at such high temperatures. However, reduced H_0 at high temperatures is consistent with the shift of the scattering weight expected from the diffuse scattering peak at (0, 0, 2) due to the nearest-neighbor AF correlations only. Therefore, $CdFe_2O_4$ seems to show very gradual dissociation of the hexagonal spin clusters with increasing temperature.

Now that $CdFe_2O_4$ nearest-neighbor correlations is found to be AF, we must admit that it is a striking departure from the FM nearest-neighbor correlations of $ZnFe_2O_4$. So what causes such a big difference between these two ferrite spinels? Structurally they show slight difference in lattice parameters ($a = 8.72$ and 8.52 Å for $CdFe_2O_4$ and $ZnFe_2O_4$, respectively) as well the Fe^{3+}-O-Fe^{3+} angles (98° and 95°). It was suggested that when Fe^{3+}-O-Fe^{3+} angle is close to 90°, the direct ferromagnetic interaction between the magnetic ions and the AF superexchange interaction through oxygen are in a subtle balance. While the direct exchange remains strong for $ZnFe_2O_4$, exchanging Zn with Cd seems enough to tip the balance in favor of AF interactions in line with Kanamori-Goodenough rule.[18,19]

Recalling that hexagonal spin clusters explained $ZnCr_2O_4$ and $CdFe_2O_4$ diffuse scattering pattern, it is also interesting to note that the essential features of $ZnFe_2O_4$ pattern can be explained using big AF hexagon clusters made of six FM tetrahedra. The calculated structure factor is

$$
\begin{aligned}
|F_{24}(\mathbf{Q})| \propto & \{\sin^2\pi h(\cos^2\pi k - \cos^2\pi l) + \sin^2\pi k(\cos^2\pi l \\
& - \cos^2\pi h) + \sin^2\pi l(\cos^2\pi h - \cos^2\pi k)\} \\
& \times \left\{ \left(1 + \cos\frac{\pi}{2}h\right)\left(1 + \cos\frac{\pi}{2}k\right)\left(1 + \cos\frac{\pi}{2}l\right) \right. \\
& \left. + \left(1 - \cos\frac{\pi}{2}h\right)\left(1 - \cos\frac{\pi}{2}k\right)\left(1 - \cos\frac{\pi}{2}l\right) \right\}. \qquad (1)
\end{aligned}
$$

Figure 5 shows the close resemblance of the experimental data and the calculated pattern. This description coincides with the RPA calculation result of the third nearest-neighbor AF interactions and the first nearest-neighbor FM interactions.[13]

The nature of the $CdFe_2O_4$ 13 K susceptibility anomaly is not completely understood yet. Broader-than-resolution diffusive elastic peaks indicate a transition to a SRO state. For $ZnCr_2O_4$, the first order structural phase transition accompanies the onset of LRO and strong local resonance.[11] However, for $CdFe_2O_4$ no structural change was identified associated with the 13 K anomaly within the limit of instrumental resolution although a weak local resonance indicative of some form of anisotropy was observed. To see whether there is any structural distortion, high resolution synchrotron x-ray scattering study will be necessary.

In conclusion, we observed $CdFe_2O_4$ inelastic magnetic neutron scattering pattern and its temperature dependence. The pattern is almost identical to that of $ZnCr_2O_4$ but is considerably different from that of $ZnFe_2O_4$. This result strongly suggests AF Fe-Fe nearest-neighbor interactions for $CdFe_2O_4$ in contrast to FM nearest-neighbor interactions found in $ZnFe_2O_4$, demonstrating tuning of 90° Fe^{3+}-O-Fe^{3+} interaction by chemical pressure. Meanwhile, the characteristic scattering pattern from the hexagonal spin clusters show surprising robustness and is observed at temperatures as high as $5\Theta_{CW}$. It is shown that these spin clusters gradually disassociate with increasing temperature when spin correlations decrease below the nearest-neighbor distance. Lastly, although spin freezing associated with the 13 K susceptibility anomaly is observed, spin dynamics does not warrant spin glass phase and no LRO is established down to 0.1 K even with 9 T vertical field applied along [001] direction.

K. K. thanks Professor K. Kohn for his advice on the single crystal growth. Work at SPINS is based upon activities supported by the NSF under Grant No. DMR-9986442.

[1] R. Ballou, E. Lelièvre-Berna, and B. Fåk, Phys. Rev. Lett. **76**, 2125 (1996).
[2] J. S. Gardner, B. D. Gaulin, A. J. Berlinsky, P. Waldron, S. R. Dunsiger, N. P. Raju, and J. E. Greedan, Phys. Rev. B **64**, 224416 (2001).
[3] M. J. P. Gingras, C. V. Stager, N. P. Raju, B. D. Gaulin, and J. E. Greedan, Phys. Rev. Lett. **78**, 947 (1997).
[4] J. S. Gardner, B. D. Gaulin, S.-H. Lee, C. Broholm, N. P. Raju, and J. E. Greedan, Phys. Rev. Lett. **83**, 211 (1999).
[5] A. Keren and J. S. Gardner, Phys. Rev. Lett. **87**, 177201 (2001).
[6] S. T. Bramwell, M. J. Harris, B. C. den Hertog, M. J. P. Gingras, J. S. Gardner, D. F. McMorrow, A. R. Wildes, A. L. Cornelius, J. D. M. Champion, R. G. Melko, and T. Fennell, Phys. Rev. Lett. **87**, 047205 (2001).
[7] S.-H. Lee, Y. Qiu, C. Broholm, Y. Ueda, and J. J. Rush, Phys. Rev. Lett. **86**, 5554 (2001).
[8] J. N. Reimers, Phys. Rev. B **45**, 7287 (1992).
[9] R. Moessner and J. T. Chalker, Phys. Rev. Lett. **80**, 2929 (1998).
[10] R. Moessner and J. T. Chalker, Phys. Rev. B **58**, 12 049 (1998).
[11] S.-H. Lee, C. Broholm, T. H. Kim, W. R. II, and S.-W. Cheong, Phys. Rev. Lett. **84**, 3718 (2000).
[12] S.-H. Lee, C. Broholm, W. Ratcliff, G. Gasparovic, Q. Huang, T. Kim, and S.-W. Cheong, Nature (London) **418**, 856 (2002).
[13] Y. Yamada, K. Kamazawa, and Y. Tsunoda, Phys. Rev. B **66**, 064401 (2002).
[14] K. Kamazawa, Y. Tsunoda, H. Kadowaki, and K. Kohn, Phys. Rev. B **68**, 024412 (2003).
[15] J. Ostoréo, A. Mauger, M. Guillot, A. Derory, M. Escorne, and A. Marchand, Phys. Rev. B **40**, 391 (1989).
[16] T. Usa, K. Kamazawa, S. Nakamura, H. Sekiya, Y. Tsunoda, K. Kohn, and M. Tanaka, in *Proceedings of the Eighth International Conference on Ferrite*, edited by M. Abe and Y. Yamazaki (Kyoto, Japan, 2000), p. 316.
[17] O. Tchernyshyov, R. Moessner, and S. L. Sondhi, Phys. Rev. Lett. **88**, 067203 (2002).
[18] J. Kanamori, J. Phys. Chem. Solids **10**, 87 (1958).
[19] J. B. Goodenough, Phys. Rev. **100**, 564 (1955).